

# Derivation of Equivalent Material Models for Composite Laminated Materials

Stanislav GOŇA, Vojtěch KŘESÁLEK

Inst. of Electrotechnics and Measurement, Tomas Bata Univ. in Zlín, Nad Stráněmi 4511, 760 05 Zlín, Czech Republic

gona@fai.utb.cz, kresalek@fai.utb.cz

**Abstract.** *In this paper, an original approach of derivation of equivalent electrical models for multilayer composite materials is presented. The purpose of the modeling is to approximate a given composite material by an equivalent dielectric slab or by a medium consisting from several dielectric layers. For each layer, an equivalent complex permittivity is set up by an optimization procedure in order to achieve the same values of reflection and transmission coefficients as are the measured values of reflection and transmission coefficients of the original composite material.*

## Keywords

Composite material, reflection and transmission coefficients, equivalent model, complex permittivity, numerical inversion.

## 1. Introduction

At the present, composite laminated materials are in widespread use in aerospace as well as in other industrial sectors. The typical composite material consists from several dielectric layers stacked together. Some layers contain partially conductive fibers (e.g. carbon ones) and are essentially anisotropic. Since existing composites contain a very dense mesh of fibers oriented in various directions, EM simulation of the reflection/transmission properties of the physical composite structure is often limited to a single periodic cell of the composite. Thus other techniques, like homogenization [1], [2], [3], [4] must be utilized to characterize composites efficiently. In homogenization approach it has been shown [1], [3] that only the 0<sup>th</sup> order (that is an average) electric and magnetic intensities can be used for a description of reflection/transmission from the composite. As a consequence the physical composite may be replaced by its homogenous equivalent.

The homogenization approach has been studied during last ten years by several authors. Specific geometries involved for example woven composites [1] and composites consisting from round partially conducting wires/fibers oriented in one direction [3]. More general

approach can be found in [4] where real life composites consisting from periodically and randomly distributed fibers were characterized. The characterization is based on a measured/simulated reflection and transmission from a composite sample and subsequent inversion of these free-space reflection and transmission coefficients into the effective permittivity. In paper [4], the effective complex permittivity was described by a smooth function of frequency. Near the first resonance, the real part of the complex permittivity changes from positive to negative values [4]. Such a behavior is characteristic for the two-dimensional array of dipoles, which show meta-properties (negative permittivity). Paper [4] also addresses important physical aspects of the equivalent modeling, such as the connection between volume concentration of the fibers and parameters of the Lorentzian dispersion law. Some other authors [5] have also presented general method of equivalent modeling, where real composite was replaced by a homogenized one layer equivalent. However in [5], only the behavior of the composite for one polarization (TE) and almost normal incidence was captured since the characterization was performed in the rectangular waveguide. Another disadvantage of the method presented in [5] is that it doesn't produce smooth functions of the complex permittivity with respect to the frequency.

In this paper reflection and transmission properties of the composites are modeled by a lossy multilayer dielectric structure. Physical properties of the structure like thicknesses of individual layers are pre-specified by a user. Electrical properties (relative permittivity and loss tangent) are then determined by a numerical optimization. The optimization seeks for optimal pairs of permittivity/loss tangent for each layer which deliver approximately the same reflection/transmission coefficients as are reflection/transmission coefficients of the measured composite sample.

The derivation of equivalent models in this paper is different from those appearing in other papers (e.g. [4], [5]) in four important aspects.

First, in our method transmission coefficients for both the orthogonal (TE) and the parallel (TM) polarization are well modeled with respect to the angle of incidence. Typically for the simplest model (based on a lossy metal) only 2 dB error for the transmission coefficient is observed for the angle of incidence 60 degrees [10] at 3 GHz.

Second, a broad range of frequencies is captured. In this paper, exemplary composites are described by smooth polynomial models for frequency range 100 MHz to 20000 MHz. The amplitude error between the original and the resultant coefficient remains below 10 dB for the entire range of frequencies, angles of incidences and polarizations.

Third, in our method only scalar measurements are performed. As information about the phase of reflection and the transmission coefficient is missing, additional constraints on the relative permittivity and loss tangent must be employed to make the inversion process unique.

Forth, our model admits only positive permittivities and is thus suitable for use with EM simulation programs.

It is interesting to see, that our models also predict correct behavior of phase of reflection and transmission coefficients. More details and frequency limitation of different models may be found in our latest paper [10].

This paper is organized as follows. In section two, investigated composite materials are described. In section three, measurement techniques and measurement results are presented. Accuracy of measurement of reflection and transmission coefficients is discussed. Modeling of composites by equivalent material models is presented in the fourth section. Conclusions are given in the fifth section.

## 2. Measured Composite Materials

In the framework of Artemis project mentioned in the acknowledgement section, three different groups of composite samples were characterized.

The first group is represented by composite samples with low shielding effectiveness (around 30 to 40 dB). The typical composite belonging to the first group is shown in Fig. 1 (on the left) and is denoted as sample B. This sample consists from a 1 mm thick pure dielectric laminate with a printed metal grid. The grid dimensions were 1.5 mm x 3 mm x 0.3 mm.

Due to the presence of the copper wire mesh with different periods in the horizontal and vertical direction, samples are essentially anisotropic. In next chapters, the following notation will be used. Symbol OkSv is used for the composite sample placed in such a way that the larger period of the copper wire mesh is oriented vertically. While OkVo stands for the situation where the composite sample is rotated by 90 degrees (larger period of the copper mesh horizontally).

The second group of samples is represented by composite laminates filled with carbon fibers. Due to the carbon filling and presence of Cu metal grid these samples show higher SE, somewhere about 60 dB at 1 GHz. As an example the sample denoted as sample 7 will be used in this paper. This sample had a physical thickness 1 mm.

As the third group of samples measured and characterized within Artemis project, composites having more complicated layer setup were studied. These composite didn't have the copper metal grid and showed shielding effectiveness between 65 to 75 dB.



Fig. 1. Measured sample B (left) and sample 7 (right). Only a small part of sample is shown to emphasize nature of a printed metal grid.

## 3. Measurement of Reflection and Transmission Coefficients

In microwave engineering it is a daily practice to perform reflection/transmission measurements to find out real and imaginary part of the complex permittivity and permeability. At microwave frequencies, these measurements are either performed on a transmission line or in a waveguide. Measured complex S-parameters S11 and S21 are then numerically inverted and complex material constants (permittivity and permeability) are obtained [6], [7]. Sometimes reflection/transmission measurements are performed in a free space under the plane wave illumination. In this case sample dimensions are required to be at least few wavelengths at the lowest frequency in order to get reflection and transmission coefficients valid for the infinite sample. Such an approach is chosen in this paper and will be described separately for reflection (section 3.1) and transmission (section 3.2). Examples of reflection and transmission measurements for two samples are given (sample B and sample 7 described earlier).

The condition that dimensions of a sample are at least few wavelengths at the lowest frequency was satisfied in our measurements at 2 or 3 GHz. At these frequencies electrical size of a sample was 2 to 3 free-space wavelengths. Since our measurement range (as mentioned later in chapter 3.1 and 3.2) was between 1-20 GHz we had to consider only measured data above 2 GHz. Missing reflection/transmission data below 2 GHz were then extrapolated from the 2-20 GHz data set (section 3.2)

### 3.1 Measurement of Reflection Coefficients

Reflection coefficients were measured in “an open test site” at school gym at UTB Zlin. An arrangement of the site is shown in Fig. 2. As receiving and transmitting antennas, broadband Vivaldi horns from RohdeSchwarz

(HE200) were used. The transmitting antenna was connected to the SMR-20 generator (Rohde-Schwarz). Received power was measured by the FSP-40 spectrum analyzer (Rohde-Schwarz). The traditional reflection measurements with a metal reference sample were performed. As the reference, 320 mm x 320 mm x 1 mm square Dural panel was used. Measured composite samples had the same transversal dimensions ( $D_x = D_y = 320$  mm). All reflection measurements were performed within 1 to 20 GHz. The maximum measurement distance for the 45 deg incidence, we could achieve due to our Gym dimensions (width 10 m), was  $R = 6$  m. For that distance a maximum frequency at which the incident field on a sample could be approximately considered as a plane wave (45 phase error on the edge of the sample) was about 14.1 GHz (See (1), Fraunhofer's distance for 45 deg incidence and maximum 45 deg phase error on edges).

$$R_{FAR\_45\text{ deg}} \cong \frac{\sqrt{2}d^2}{\lambda_{\min}} \quad (1)$$

Due to the arrangement of the test site, reflections from walls of the gym were kept at relatively low level (less than minus 30 dB) and relatively high dynamic range of reflection measurements was achieved (see Fig. 3). Due to the fact that samples had dimensions of 20 wavelengths at the highest frequency (20 GHz), the position of the Rx and Tx Vivaldi horns had to be precisely set by a laser distance meter from Leica company.

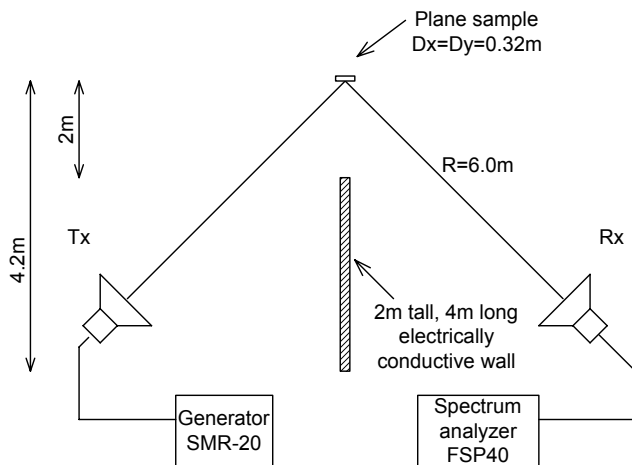


Fig. 2. Reflection measurements – Arrangement of the test site.

An example of measured reflection coefficients  $R_{11}$  and  $R_{22}$  for sample B is shown in Fig. 3. The reflection coefficients show an anisotropy in the horizontal and the vertical planes. The anisotropy is removed by averaging of  $R_{11}$  and  $R_{22}$  expressed in dB. The sample B (and also other composite samples measured within project Artemis) show almost perfect reflection from the smooth side. On the other hand, the rough side is less reflective at high frequencies. For definition smooth – rough side see Fig. 12.

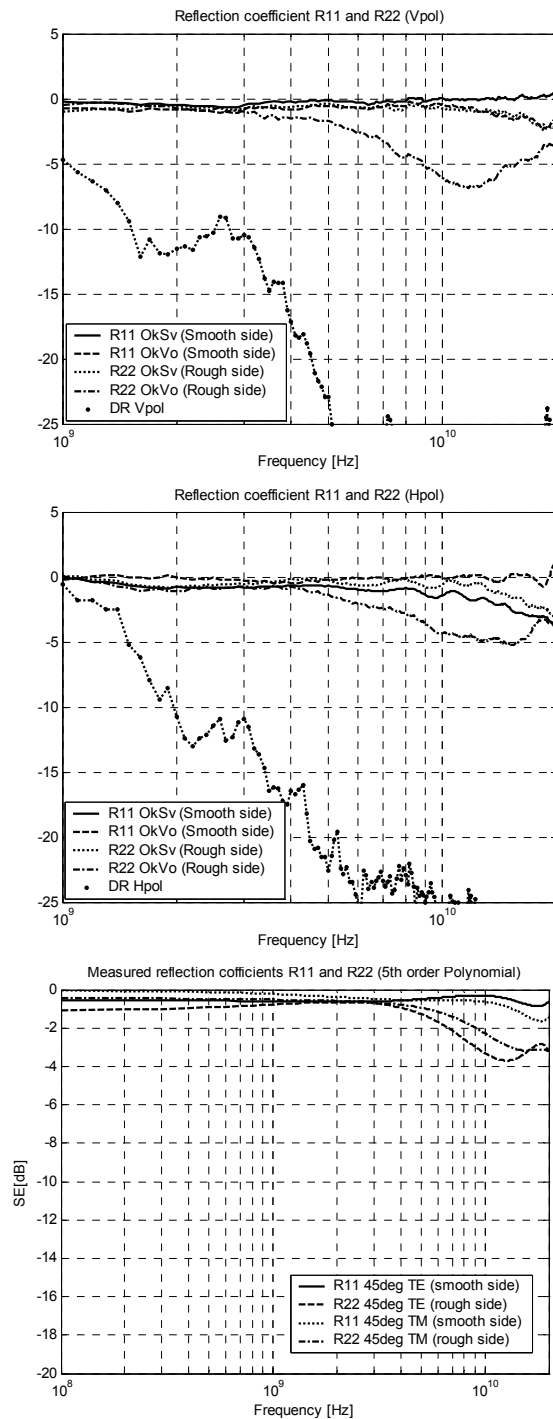


Fig. 3. Top) Measured reflection coefficients (Sample B) Bottom) After removing anisotropy by averaging of  $R_{11OkSv}$  and  $R_{11OkVo}$ , resp.  $R_{22OkSv}$  and  $R_{22OkVo}$ . DR Vpol and DR Hpol stand for the available dynamic range in our test site.

### 3.2 Measurement of Shielding Effectiveness

Electromagnetic characterization of composite materials is often limited to measurement of the overall shielding effectiveness. Practically shielding effectiveness is either tested for the far field plane wave illumination or measured by a set of near field magnetic probes (loop antennas). If values of shielding effectiveness for these two

cases are compared, lower shielding effectiveness is always obtained if measured by near field magnetic probes. This is because near field magnetic component penetrates the tested material more easily than the electric one. Such a measurement then represents the worst case in SE measurements.

In this paper it is assumed the composite under test is illuminated by a plane wave and the composite is within the far field region of the plane wave source. Then, the shielding effectiveness for both the E and H field component is the same. Next assumption is that dimensions of a composite sample are at least few wavelengths along the x and y axis. In such a case “true plane wave reflection and transmission” occurs in the sample. Finally, last assumption is that there is only a forward wave penetration through the sample and no side (along the edges propagation) occurs. To neglect this side propagation along the sample, “on wall approach is being used”. Our experimental setup being used during measurements of the shielding effectiveness of composite materials is shown in Fig. 4.



Fig. 4. Transmission measurements – Shielded box with sample 7 attached.

A sample under test is placed on a front wall of a shielded rectangular test box (chamber). Box dimensions were 600 mm x 500 mm x 500 mm. The box with a sample attached is illuminated by a plane wave produced by the transmitting Vivaldi horn antenna (HE200 from Rohde-Schwarz). The same horn is placed inside the box and acts as a receiving antenna. The aperture of the receiving antenna was 1 cm behind the sample. The shielded box was manufactured from a stainless steel and had a remountable front cover. The cover was electrically connected with the box by a series of Lairtech fingerstocks. Attachment of a sample was realized by four L-shaped sliders. The sliders provided strong and equally distributed press force and ensured minimal sample to cover air-gaps. In order to check the cover to wall connection, measurement of the shielding effectiveness of the box with 320 mm x 320 mm Dural panel mounted on the front was performed. Typical shielding effectiveness at 2 GHz was around 85 dB which was sufficient for measured composites as they showed the SE between 65 to 75 dB at 2 GHz. In order to damp resonances within the box, a pyramidal absorber was made. The absorber consisted from 16 pyramids, each 200 mm long. Pyramids were made at UTB and had a wooden core coated by a 2.2 mm thick lossy rubber. This rubber was developed at UTB in the past for reducing RCS of aircrafts.

Measurements of shielding effectiveness were per-

formed in two steps. First, a sample was removed and the power  $P_{air}$  delivered by the receiving horn was measured. Then sample was attached to a wall with the aid of four sliders and the power  $P_{sample}$  was obtained. Shielding effectiveness (SE) was then

$$SE = P_{air} - P_{sample} \quad (2)$$

Measurement of the shielding effectiveness was performed within the range 1 to 20 GHz. Examples for measured SE for samples B and 7 are given in Figs 5, 6 and 7.

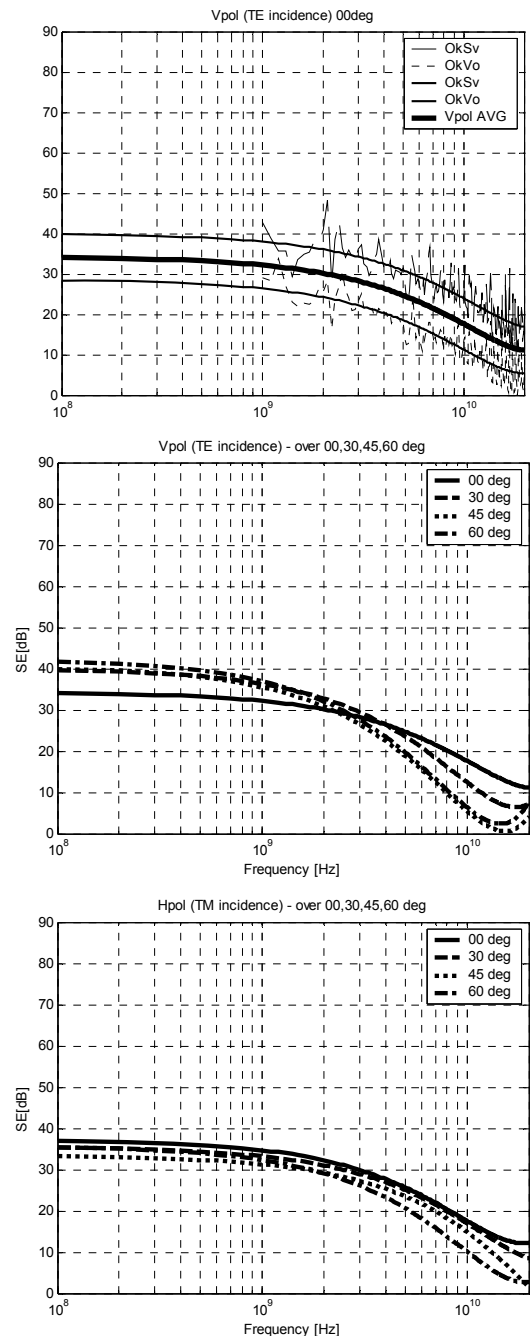


Fig. 5. Measured shielding effectiveness of Sample B (top graph) - normal incidence 00 deg, effect of anisotropy (middle graph) Oblique incidence (Vpol), anisotropy removed by averaging between planes OkSv and OkVo (bottom graph) Oblique incidence (Hpol).

According to Fig. 5, shielding effectiveness of sample B is around 30 to 40 dB at 1 GHz, depending on the angle of incidence and polarization. As frequency increases sample B becomes more transparent for EM waves. The first null of the transmission coefficient (serial resonant frequency  $f_s$ ) occurs between 20 to 30 GHz. Our closer prediction of that frequency via in house MoM code for numerical analysis of reflection/transmission properties of frequency selective surfaces predicts  $f_s = 23$  GHz.

The SE data given in Fig. 6 are valid for the normal incidence and illustrate the effect of sample anisotropy (different SE in different planes/samples orientation). The SE data for a sample oriented according to Fig. 1 (horizontally placed sample) are denoted as OkSv, while the SE data for a sample rotated by 90 deg are denoted as OkVo. Actual SE measurements were performed within 1-20 GHz range. The SE data down to 100 MHz were obtained by extrapolation.

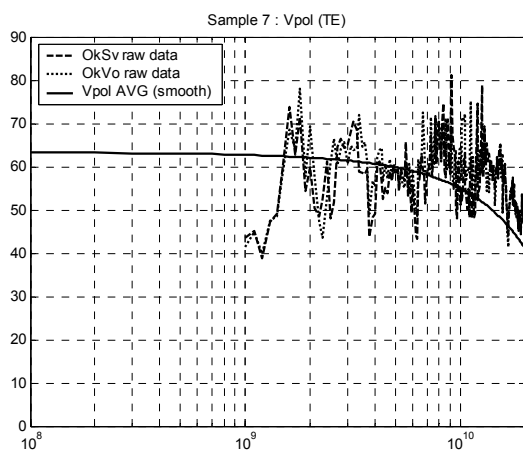


Fig. 6. Measured shielding effectiveness of Sample 7 (VERTICAL POLARIZATION) – SE data for OkSv and OkVo differs due to anisotropy. For setting up an equivalent model, anisotropy is removed by averaging of OkSv and OkVo and neglecting SE data below 2 GHz.

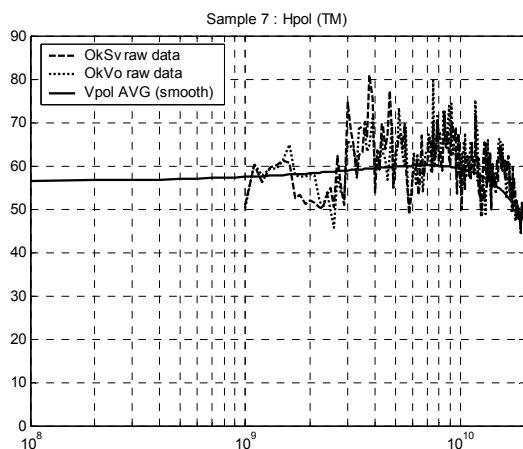


Fig. 7. Measured shielding effectiveness of Sample 7 (HORIZONTAL POLARIZATION).

Measurement of shielding effectiveness of sample 7 was done similarly as for sample B (Figs. 6 and 7). For

each polarization (TE or TM) shielding effectiveness for both OkSv and OkVo planes are given. Their average is then approximated by a polynomial and this smooth curves are denoted by  $T^{TE}_{orig}$  and  $T^{TM}_{orig}$  transmission coefficients. These coefficients were used during generation of the equivalent models (preprocessing). The SE data for the vertical polarization show significant fallouts (drops) at 1.3, 2.2, 3.8 and 6.3 GHz. These drops in the SE curve were caused by existing air gaps between the sample and the cover of the PEC box. Levels of these drops were between -25 dB (1.3 GHz) to -15 dB (6.3 GHz). These drops could be reduced if a greater overlap of the sample and the cover of the PEC box is used. In our case, all measured samples had an overlap 30 mm. The influence of a sample to cover air gaps was much less evident for the horizontal polarization (see. Fig. 7).

### 3.3 Measurement Accuracy

Power measurement errors for the generator SMR-20 and the spectral analyzer FSP40 is maximally 0.5 dB. Repeatability of measurements with respect to the mounting and dismounting sample was around 1 dB. Thus, overall measurement error for reflection and transmission coefficients may be estimated around 2 dB.

Except of power measurement errors, for frequencies above 14 GHz, systematic (that is errors linked with measurement method) were introduced, since the necessary Fraunhofer's distance was not satisfied. At frequencies about 20 GHz, the additional systematic error can be estimated around 1 dB.

## 4. Equivalent Model

This section will mathematically describe the procedure of derivation of an equivalent model for a measured composite sample. Let's consider a situation according to Fig. 8. The measured composite sample is characterized by its reflection/transmission coefficients. Since equivalent models are intended for use with fullwave EM simulation programs with a focus to shielding effectiveness (SE) calculations, primarily accurate modeling of transmission coefficients is required. On the other hand, modeling of reflection behavior is less critical and in some cases is not considered (but it is fulfilled automatically, see one layer model based on lossy metal in section 4.1). A typical example includes the evaluation of the shielding effectiveness (SE) of an aircraft at lower frequencies where all composites show almost perfect reflection and high insertion loss (typically 40 to 75 dB).

Since the behavior of the SE is of primary interest, an accurate measurement of transmission coefficients for an oblique incidence must be performed. In our experimental setup (previously described in section 3) measurements for 0, 30, 45 and 60 degrees were considered.

During setup of an equivalent model it is necessary to find a suitable equivalent complex permittivity of the indi-

vidual dielectric layers to meet a correspondence between measured coefficients (denoted by ORIG suffix) and the coefficients predicted by the model (suffix RES, meaning resultant).

As shown in Fig. 8, the measured data set contains both reflection and transmission coefficients. Indexes TM and TE are being used for a polarization parallel with the plane of incidence and the polarization orthogonal to that plane. In our measurement setup, parallel polarization corresponded to the horizontal polarization while the orthogonal one was identical with the vertical polarization.

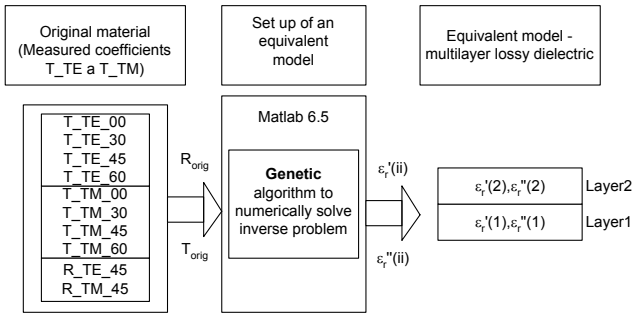


**Fig. 8.** Determination of a complex permittivity for an equivalent model (Inverse problem solved by genetic algorithms).

In order to explain setting up of an equivalent model, let's consider that we are only interested in the normal incidence (model for oblique incidence will be described in section 4.1).

Our measured data set contains reflection coefficients for the 45 deg incidence since we didn't have a network analyzer or a directional coupler. Thus reflection measurements were done with the aid of PEC wall to separate Rx and Tx antennas. See details in section 2.

The relation between reflection and transmission coefficients and complex permittivities of dielectric layers is described by functions  $f_R^{TE}$ ,  $f_R^{TM}$ ,  $f_T^{TE}$ , and  $f_T^{TM}$ . These functions represent the well known Fresnel reflection/transmission coefficients. An example of the functions for the one and the two layer dielectric structure is given in Appendix A (notation according to book [9] was used).

$$R^{TE} = f_R^{TE}(\varepsilon'_{r1}, \varepsilon''_{r1}, \varepsilon'_{r2}, \varepsilon''_{r2}, \dots), \quad (3a)$$

$$R^{TM} = f_R^{TM}(\varepsilon'_{r1}, \varepsilon''_{r1}, \varepsilon'_{r2}, \varepsilon''_{r2}, \dots), \quad (3b)$$

$$T^{TE} = f_T^{TE}(\varepsilon'_{r1}, \varepsilon''_{r1}, \varepsilon'_{r2}, \varepsilon''_{r2}, \dots), \quad (3c)$$

$$T^{TM} = f_T^{TM}(\varepsilon'_{r1}, \varepsilon''_{r1}, \varepsilon'_{r2}, \varepsilon''_{r2}, \dots) \quad (3d)$$

where  $\varepsilon'_{r1}$  and  $\varepsilon''_{r1}$  account for the real and the imaginary part of permittivity of the first dielectric layer.

$$\varepsilon'_r = \varepsilon_r, \quad (4a)$$

$$\varepsilon''_r = \varepsilon_r \cdot \text{tg} \delta \quad (4b)$$

Equations (3a) to (3d) represent four complex equations (or 8 real ones). Each equation depends on complex permittivities of dielectric layers. To solve equations (3a) to (3d) uniquely, the same number of equations as the number unknowns is needed. For example, for non magnetic model, the four layer dielectric structure would have to be used to solve equations (3a) to (3d) uniquely (in case that the sample under test is a true lossy multilayer dielectric and has no wires/ fibers within).

Determination of the complex permittivity of the dielectric samples consisting from a single lossy dielectric layer is a common task for material/microwave engineers. In this situation, the most simple and popular is reflection measurement within the short-ended waveguide or the transmission line [6]. Then, only the equation (3a) is considered and upon the measured complex reflection coefficient, the permittivity and loss tangent of a sample is uniquely determined.

It is also possible consider the equivalent model having both complex permittivity and permeability [7], [8]. Then twice less equivalent layers is necessary, but this model is computationally inefficient, as real relative part of the complex permittivity and the complex permeability greater than one result in a dense FDTD mesh.

In our case the solution of equations (3a) to (3d) is complicated by two facts. First, equations (3a) to (3d) cannot be solved implicitly because of the transcendent character of functions  $f_R^{TE}$ ,  $f_R^{TM}$ ,  $f_T^{TE}$ , and  $f_T^{TM}$ . That's why the numerical solution via an optimization method has to be employed. Simple permittivity measurement of dielectric samples (such as the one used in [6]) relies on the local optimization via Quasi Newton method. Second, we often have less equation than unknowns. Then, solution of equations (3a) to (3d) can only be made approximately. In this case local techniques (e.g. Quasi-Newton method) are used to obtain a solution (projection) in a least square sense. Another, more versatile technique is utilization of the genetic algorithms (GA) described in next section.

#### 4.1 Setting up of an Equivalent One Layer Model by GA

In this section examples of setting up of an equivalent model for composite samples B and 7 are given.

In general, equivalent models are required to fulfill these attributes

- The model must accurately predict behavior of the  $T^{TM}$  (parallel) and the  $T^{TE}$  (orthogonal) coefficients versus large angle of incidences.
- Broadband behavior of coefficients  $T^{TM}$  and  $T^{TE}$  must be ensured. Both the real part of the complex permittivity and the loss tangent must be described by simple smooth functions (ideally polynomials) with frequency as the independent parameter.

- The model must be numerically efficient; this is only ensured when a contraction factor of each layer is kept low. Thus only a small real part of permittivity (or permeability) is admissible.
- If possible, the model should roughly predict the reflection from a measured composite sample.

Let's now turn our attention to the derivation of the equivalent model with a single dielectric layer. The following series of steps is performed

- Measured transmission coefficients  $T^{TM}$  and  $T^{TE}$  are preprocessed. First, for each polarization (TM or TE) and the angle of incidence, measured dB values of the transmission coefficients for planes OkSv and OkVo are averaged and thus the anisotropy is removed. Then frequency dependence of the  $T^{TE}$  and the  $T^{TM}$  coefficients is approximated by a smooth function. In our case, a second-order polynomial was sufficient, since the decrease of an average shielding effectiveness with the frequency was relatively smooth and monotonic. Approximation by the second order polynomial proved to be also sufficient for extrapolation of the SE data down from 1 GHz to 100 MHz.
- As the second step, series of equations (3a) to (3d) is solved approximately by the binary coded genetic algorithms. Prior running the GA, the following cost function is assembled

$$\begin{aligned} Cost = & \sum_{ii=00}^{60} ((T_{orig,ii}^{TE} - T_{res,ii}^{TE})^2) \\ & + \sum_{ii=00}^{60} (T_{orig,ii}^{TM} - T_{res,ii}^{TM})^2 \end{aligned} \quad (5)$$

where double index  $ii$  represents discrete incident angles (00, 30, 45 and 60 deg). Symbols  $T_{orig}^{TE}$  (resp.  $T_{orig}^{TM}$ ) and  $T_{res}^{TE}$  (resp.  $T_{res}^{TM}$ ) stand for the original (measured) and the resultant (after finishing GA optimization) transmission coefficient. Details about the structure of one chromosome, number of genes (parameters) and number of bits per gene are described in section 4.1.1.

- After running the GA, equivalent complex permittivity (in our case real part permittivity and loss tangent) for each frequency is stored. Since GA is a stochastic technique, each GA run produces a different value of complex permittivity. To reduce the variation, at each frequency, GA optimization is run few times (e.g. 5 times in our code) and only the run having lowest cost function is further considered. Thus random oscillation of complex permittivity with frequency is minimized. It has been observed that the maximal error between the measured (orig) and resultant (res) transmission coefficients is less than 10 dB.

It has been found that for the purpose of prediction of shielding effectiveness of a composite for further use

in fullwave EM codes, even a very simple approximation of the composite was adequate. This approximation considered the real part of permittivity equal to one and leaving only the loss tangent variable. This approximation will be called as a LOSSY METAL. Usage of this simple model typically results in 5 dB error between the (orig) and (res) coefficients at lower frequencies. Thus, a very good agreement in terms of EMC measurement accuracy is achieved.

- Finally, a table given frequency dependence of complex permittivity (let's call this as DISCRETE DATA SET) is approximated by a smooth function. In our case the third order polynomial proved to be sufficient to express permittivity/loss tangent accurately within the frequency range 100 to 20000 MHz.

$$tgdel = 10^{P_3 \cdot X^3 + P_2 \cdot X^2 + P_1 \cdot X + P_0} \quad (6)$$

where coefficients  $P_0$ ,  $P_1$ ,  $P_2$  and  $P_3$  are obtained by application of Matlab `polyfit.m` function on the discrete loss tangent data set.

In order to check the prediction of shielding effectiveness by the DISCRETE DATA SET and by the smooth approximation, coefficients  $T^{TM}$  and  $T^{TE}$  are recalculated for the smooth approximation and SE results are compared with those predicted by a discrete data set.

#### 4.1.1 Examples for Model B and Model 7

Let's now turn our attention to the examples of equivalent models for composite materials B and 7. Model 7 will be described in detail, for model B only the resultant loss tangent is given. The procedure of derivation of both models was the same and corresponded to a list of steps described in the previous sections. Fig. 9 shows the result of the GA inversion where the original (measured) transmission coefficients  $T_{orig}^{TM}$  and  $T_{orig}^{TE}$  are compared with the coefficients predicted by the one layer model. In the same figure, the maximum error between measured transmission coefficients and the coefficients predicted by the model is shown. The error is around 7 dB for 45 deg angle of incidence. The numerical inversion via GA assumed only one variable parameter (loss tangent). The parameter was coded by 32 bit long word and at each GA iteration, 48 individuals were used. Typically, 3 to 5 iterations were needed to reach the global minimum.

In next figure (Fig. 10), the smooth one layer model is given where the loss tangent is approximated by the third order polynomial. In the same graph, agreement between the model produced directly by GA and the smooth model is compared. It can be seen, that the models differ less than 3 dB.

Finally, the last figure (Fig. 11) shows the comparison of the loss tangent for the one layer model for model 7 and model B.

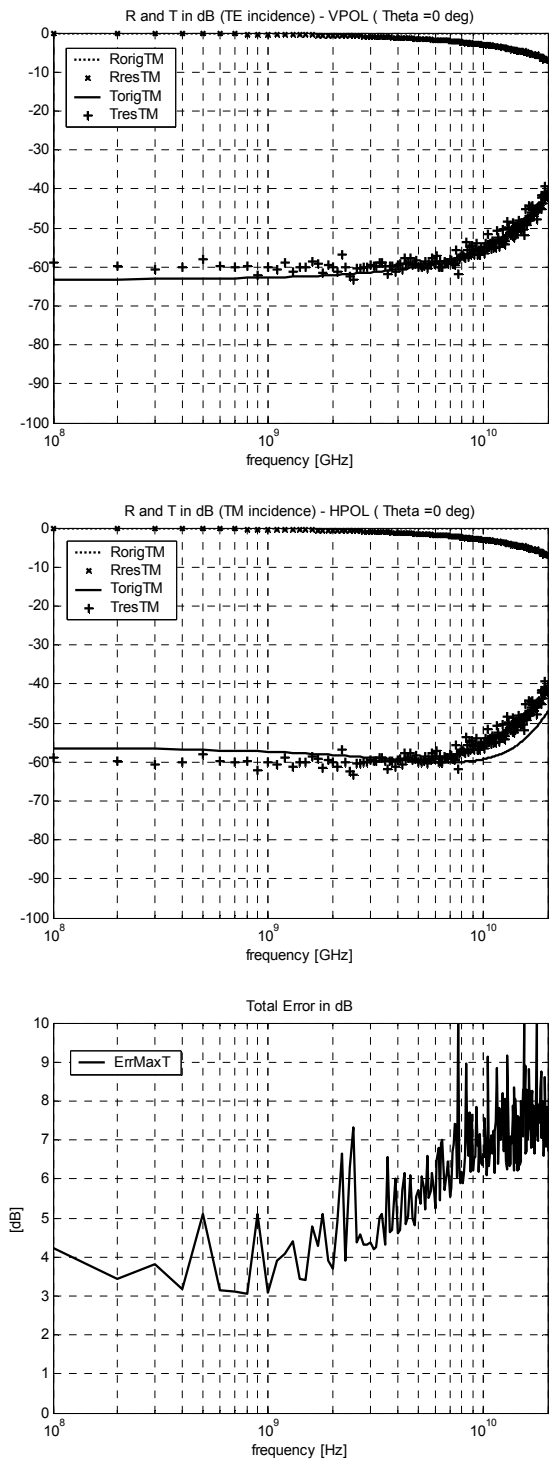


Fig. 9. Replacement of composite sample 7 by the one layer equivalent model (LOSSY METAL). Top two graphs: Transmission coefficients obtained after running GA (discrete data set). Only results for 45 degree incidence are shown. Bottom graph: The error between the original - measured (ORIG) and the resultant (RES) - model predicted (angle of incidence up to 60deg) transmission coefficients.

### 4.1.2 One Layer Model - Conclusions

The one layer model presented in previous section was based on a lossy metal. This model is computationally

efficient for use with EM simulation programs and provides amplitude accuracy of modeling transmission coefficient better than 10 dB up to 20 GHz. The accuracy of prediction of the reflection coefficient is around 5 dB for 3 GHz [10].

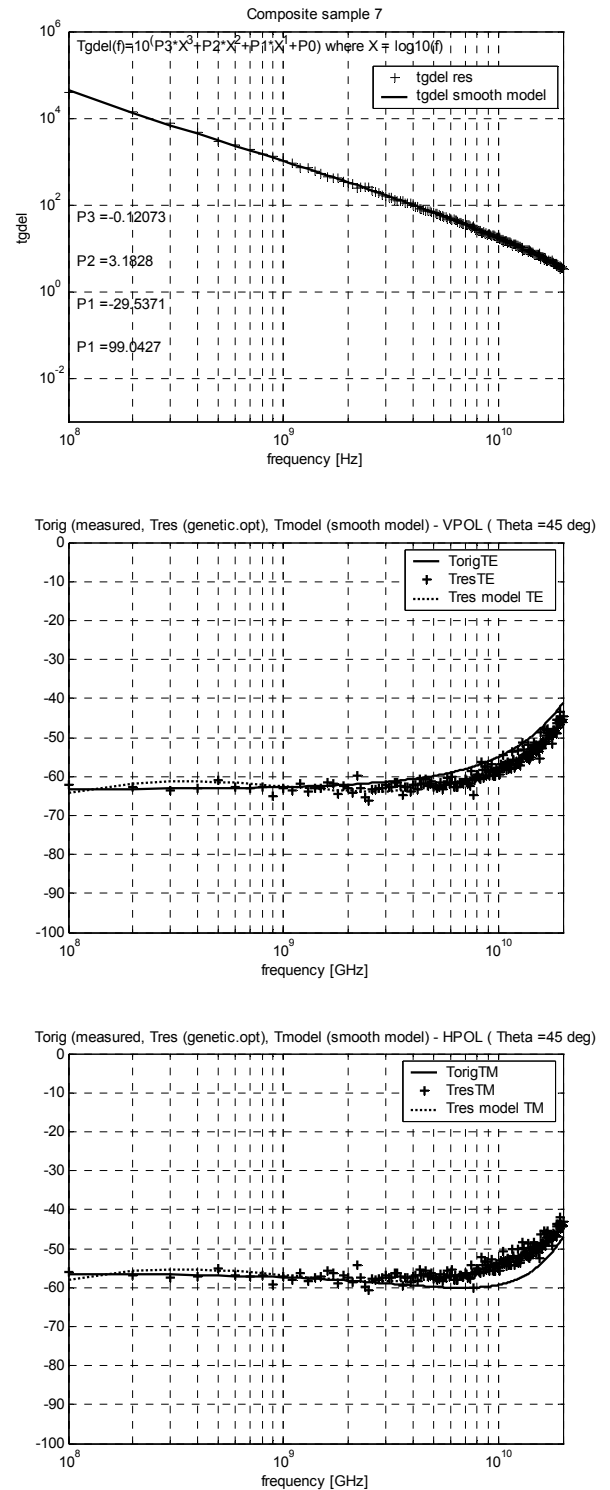


Fig. 10. Example of the one layer equivalent model for composite 7 (LOSSY METAL),  $t_1 = 10$  mm. Top graph: Frequency dependence of loss tangent. Bottom graph: The agreement between discrete and smooth model for loss tangent.



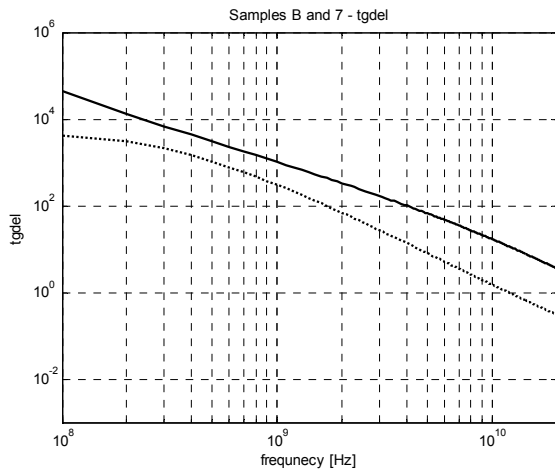


Fig. 11. Loss tangent for sample B (dashed) and sample 7 (solid), one layer model – lossy metal),  $t_1 = 10$  mm.

## 4.2 Two Layer Equivalent Model

In this subsection, derivation of a two layer model for the composite sample B will be described. The model assumes that both relative permittivity and loss tangent of the first and second dielectric layer are variable. Thus, in total we have 4 independent variables for tuning R/T characteristics of the two layer model. Therefore both transmission and reflection from the sample B may be modeled with the model quite accurately (as shown in subsequent paragraphs). Before describing derivation of the two layer model by GA, let's explain first a physical arrangement of the composite B and its transmission/reflection behavior.

A decision about the physical nature of the composite sample prior running numerical inversion via GA must be performed as we have an underdetermined problem (scalar R/T measurements instead of vector ones) and additional constraints on permittivity and loss tangent must be considered to make the inversion process unique.

The composite sample B consists from a Cu grid printed on a laminate (having permittivity around 5.0 and thickness 1 mm). Let's denote the side with Cu grid as a smooth one. From this side, the composite is almost perfectly reflecting (see. Fig. 12). The other (second) side of the composite will be denoted as a rough one. When looking for the reflection coefficient  $R_{22}$  from this side, we observe only partial reflection due to low permittivity of the laminate and due to a certain moderate loss tangent of the laminate. Thus we encounter an asymmetry in reflection coefficients  $R_{11}$  and  $R_{22}$ . It has been found, that in the simplest case, the two layer structure may accurately model the asymmetry. The most straightforward solution is to take high relative permittivity and loss tangent of the first layer and leave the relative permittivity of the second layer low to maintain  $R_{22} < 1$ . Loss tangent of the second layer must be substantially high to appropriately absorb the wave incident on the rough side.

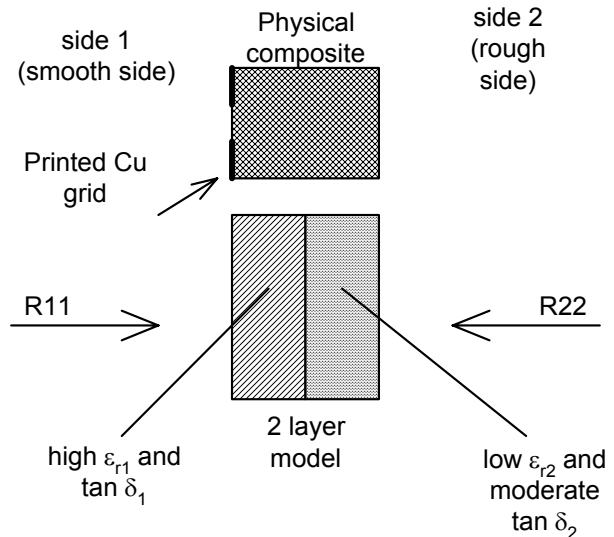


Fig. 12. Two layer model ( $t_1 = t_2 = 5$  mm). Asymmetry in reflection coefficients  $R_{11}$  and  $R_{22}$  is modeled with a given combination of  $\epsilon_{R1}$ ,  $\epsilon_{R2}$ ,  $\tan \delta_1$  and  $\tan \delta_2$ .

Transmission characteristics of the composite sample B are plotted in Fig. 5, where measured shielding effectiveness for angles of incidence from 0 to 60 deg is given. From the graphs in Fig. 5, it can be concluded that up to frequency 3 GHz, the TM and TE transmission through the composite sample shows increase of the  $T^{TM}$  coefficient with increasing angle of the incidence while the  $T^{TE}$  coefficients tend to decrease with the angle of incidence. Such a behavior is the same as the one known for a single dielectric slab (if the angle of incidence is less than the Brewster's angle). Thus, the one layer model may accurately model transmission through the composite for lower frequencies (low frequency approximation). At higher frequencies the one layer model is less accurate but the measured transmission coefficients do not vary with the angle of incidence too much. Therefore, even at higher frequencies (up to 20 GHz), the one layer model may guarantee maximal approximation error well below 10 dB which is a sufficient value in prediction of shielding effectiveness of an object (like an aircraft) within the EM simulation program (e.g. FDTD one).

Let's now turn our attention to the derivation of the two-layer equivalent model for sample B. The derivation was done with the aid of genetic algorithms and assumed that we have 4 independent variables (relative permittivity of the first and second layer and their loss tangents). The relative permittivity of both layers was constrained from 1 to 100. The loss tangent was limited from 0.0001 to 10000. Physical thickness of both layers was set to the same value ( $t_1 = t_2 = 5$  mm). In the criterial function (7), both  $R$  and  $T$  coefficients were considered. The resultant relative permittivity of both layers and loss tangent were modeled by the 3<sup>rd</sup> order polynomials with coefficients  $P_i$  and  $D_i$  given by equations (8a) and (8b).

$$Cost = \sum_{ii=00}^{60} ((T_{orig,ii}^{TE} - T_{res,ii}^{TE})^2) + \sum_{ii=00}^{60} (T_{orig,ii}^{TM} - T_{res,ii}^{TM})^2 + (R11_{orig,45}^{TE} - R11_{res,45}^{TE})^2 + (R22_{orig,45}^{TE} - R22_{res,45}^{TE})^2 + (R11_{orig,45}^{TM} - R11_{res,45}^{TM})^2 + (R22_{orig,45}^{TM} - R22_{res,45}^{TM})^2 \tag{7}$$

$$\epsilon_R = \sum_{i=0}^3 P_i X^i, \tag{8a}$$

$$\tan \delta = 10 \left( \sum_{i=0}^3 D_i X^i \right), \tag{8b}$$

$$X = \log_{10}(f). \tag{8c}$$

### 4.2.1 GA Inversion – Implementation Notes

To successfully obtain unknown permittivity and loss tangent of the first and second dielectric layer, GA inversion must be performed with additional constraints to make the inversion uniquely determined.

$$\epsilon_{R1} > \epsilon_{R2}, \dots \tag{9a}$$

$$\tan \delta_2 > \tan \delta_1, \dots \tag{9b}$$

$$\epsilon_R < \epsilon_{R \max}(f). \tag{9b}$$

Constraints (9a) and (9b) were derived upon a physical insight into reflection/transmission behavior of the two layer composite described in Fig. 12. Values of constraint (9c) on a maximum relative permittivity were found by running the GA for a lossless case ( $\tan \delta_1 = \tan \delta_2 = 0$ ) where only  $\epsilon_{R1}$  and  $\epsilon_{R2}$  are tuned to achieve the measured reflection coefficients (Fig. 13).

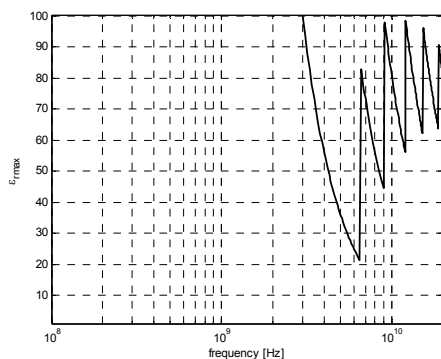


Fig. 13. 2D GA inversion – maximum limit on relative permittivity of the first and second dielectric layer.

In order to make simple approximation of the complex permittivity versus frequency, frequency range 100 to

20000 MHz was splitted into 7 frequency intervals. These intervals correspond to the first, second, third or higher order resonance thickness of the single dielectric slab with  $t = 10$  mm.

- Interval 1: 0.1 – 1.5 GHz, Interval 2: 1.6 – 6.5 GHz
- Interval 3: 6.6 – 9.0 GHz, Interval 4: 9.1 – 11.8 GHz
- Interval 5: 11.9 – 15.2 GHz, Interval 6: 15.3 – 18.8 GHz
- Interval 7: 18.8 – 20.0 GHz

In each frequency interval both the permittivity and the loss tangent of the first and second dielectric layer are approximated by 3<sup>rd</sup> order polynomials (8a) and (8b).

With constrains (9a), (9b) and (9c) being applied during GA run, the following resultant reflection and transmission coefficients were obtained (Fig. 14).

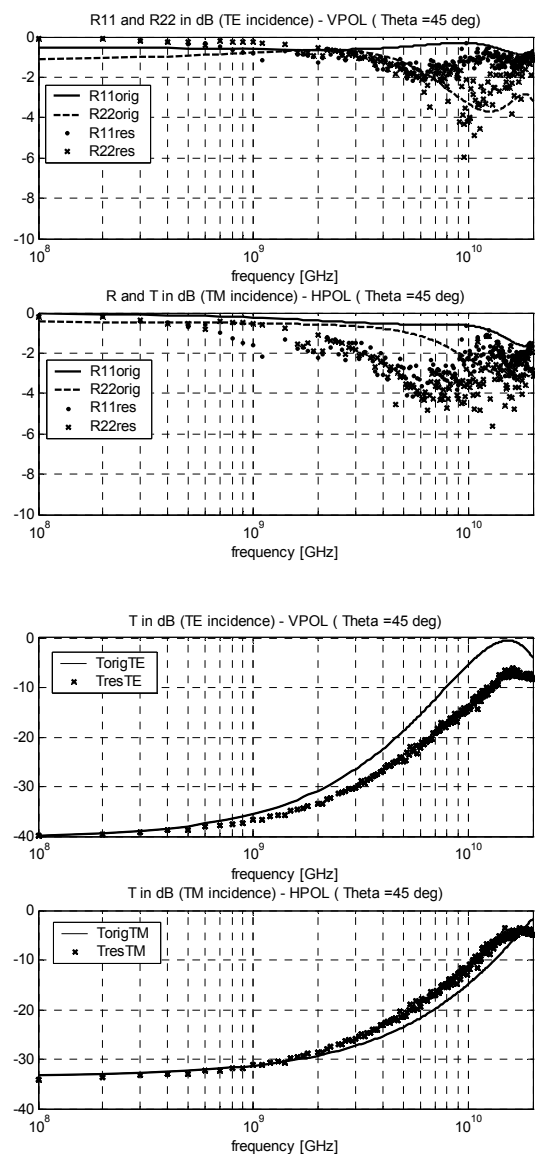
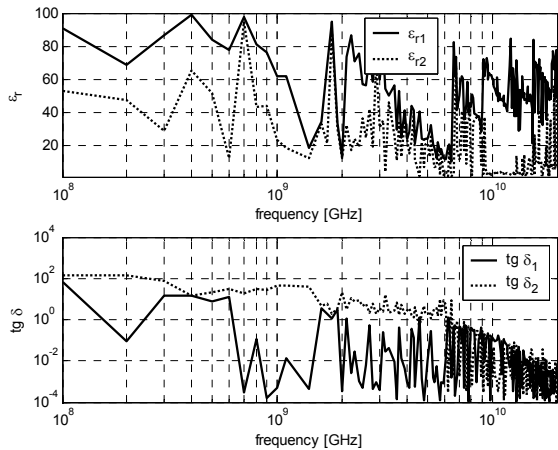
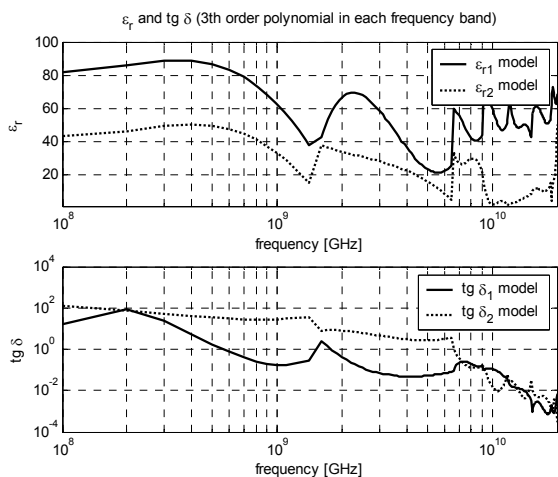


Fig. 14. Two layer model ( $t_1 = t_2 = 5$  mm) – Resulting (res) and Original (measured) reflection and transmission coefficients.

The resultant complex permittivity of the two layer model is given in Fig. 15. It can be seen that the frequency dependence of the loss tangent is reasonably smooth monotonically decreasing function. On the other hand, the relative permittivity tends to change with frequency in a difficult manner. This change is theoretically almost linear but whenever GA inversion bounces on  $\varepsilon_{Rmax}$  limit, then the other branch of solution of the transcendental like equation describing our two layer problem, is chosen. Results of the smooth approximation are shown graphically in Fig. 16. Tabular representation of the results (coefficients  $P$  and  $D$  from equations (8a) and (8b)) is given in Tab. 1.



**Fig. 15.** Two layer model ( $t_1 = t_2 = 5$  mm) for sample B: Permittivity and loss tangent of the first and second dielectric layer obtained by GA with constraints (9a), (9b) and (9c) applied. During GA the following attributes were used: 4 genes (variable parameters), each coded by 48 bits, population of 192 individuals, probability of crossover = 1.0, probability of mutation 0.05.



**Fig. 16.** Final smooth approximation for complex permittivity of 2-layer model for sample B.

## 4.2.2 Approximation Errors

We have observed that the maximal error for the transmission coefficient was about 7 to 10 dB (see Fig. 17). This error is valid for the whole range of frequencies between 100-20000 MHz and all considered angles of incidence (0 to 60 deg).

The maximum of the error for reflection coefficient is about 3 dB. The high value of MaxErrT is mainly influenced by a larger measurement error for reflection coefficients in our experimental setup (due to the violation of (1)). We have also tested the generation of the equivalent two layer model on a synthetic R/T data produced for sample B with the aid of our house periodic MoM code called FSS1R. In this case, a maximum error MaxErrR and MaxErrT less than 3 dB could be achieved.

$P$	$\varepsilon_1$	$\varepsilon_2$	$D$	$\tan \delta_1$	$\tan \delta_2$
$P_0$	56600.10	48164.61	$D_0$	-6855.31	-624.32
$P_1$	-20527.57	-17392.59	$D_1$	2394.68	225.72
$P_2$	2482.86	2394.68	$D_2$	-278.20	-27.01
$P_3$	-100.00	-83.88	$D_3$	10.75	1.07

**Tab. 1.** Resultant polynomial coefficients for relative permittivity and loss tangent of the two layer model for sample B (Interval 0.1-1.5 GHz).

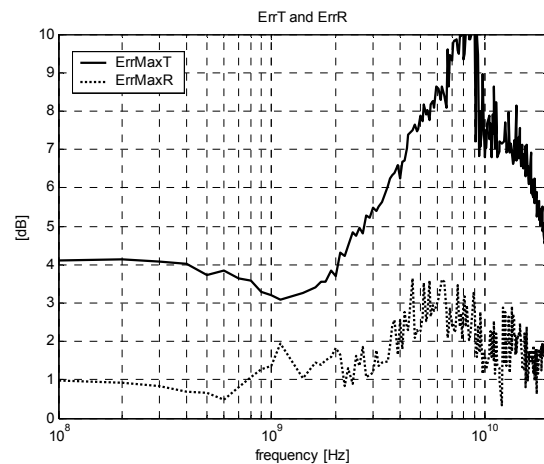


**Fig. 17.** Maximal errors for reflection and transmission coefficient for sample B.

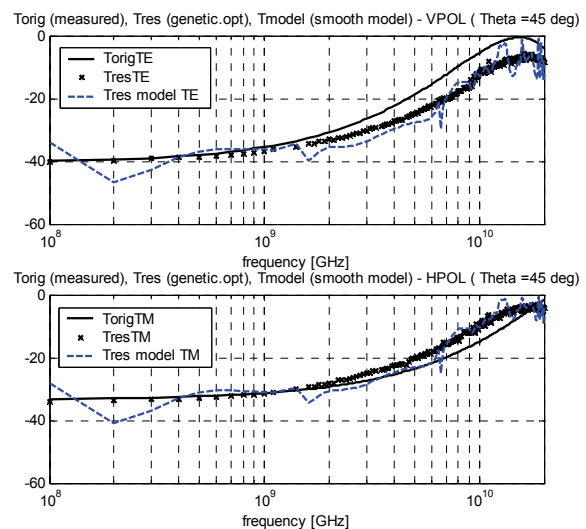


**Fig. 18.** Verification of smooth model for sample B.

Finally, the last step in deriving the equivalent two layer model for sample B was to check how accurately the smooth functions for  $\varepsilon_{R1}$ ,  $\varepsilon_{R2}$ ,  $\tan \delta_1$ ,  $\tan \delta_2$  represent resul-

tant R/T coefficients. The comparison is shown in Fig. 17, where the approximation error is about 5 dB for the  $T^{\text{TE}}$  coefficient and around 5 dB for the  $T^{\text{TM}}$  one, if considering frequencies above 1 GHz.

### 4.3 Validation of Equivalent Models

The developed equivalent models were validated by the FDTD simulation of a small aircraft [11]. The simulations were performed up to 3 GHz and an agreement between the model predicted and measured shielding effectiveness at different points of interest inside the plane was typically less than 10 dB. The two layer model was validated only against the synthetic R and T data produced by our in-house periodic MoM code called FSS1R. More details about the accuracy of the two layer model can be found in [10].

## 5. Conclusions

In this paper, the one and the two layer equivalent model consisting from a non-magnetic, lossy dielectric structure was presented. The one layer model is sufficient if only transmission properties of the composite are of interest while the two layer model may predict reflection properties of the composite sample, including  $R_{11}$  and  $R_{22}$  asymmetry. All models were derived upon the measured reflection and transmission coefficients for the physical composite samples. These models are valid in frequency range 100 MHz to 20000 MHz and exhibit maximum error for transmission and reflection coefficient below 10 dB. The error is also valid for large range of angles of incidences (0 to 60 deg).

The one layer model is based only on the lossy metal and is extremely efficient for use with the full-wave EM simulation programs (e.g. FDTD). The two layer model assumes that the real permittivity of any layer falls into range 1 to 100. Both, the one and the two layer model assume very high loss tangent at low frequencies. Typically, equivalent conductivity is around 5000 S/m at 1 GHz ( $SE = 60$  dB).

All models derived in the paper assume that the components of the complex permittivity are represented by smooth polynomial functions. Therefore, the models may be easily used with both the time and the frequency domain EM simulation programs.

## Acknowledgements

The research described in the paper was financially supported by the Czech Ministry of Trade and Industry under project ARTEMIS "Research of Efficient Methods of Preparation of Models for Composite Aircraft for Analysis of its Exposure by Electromagnetic Interference from the Environment". Grant No. FT-TA4/043 (2007-2010, MPO/FT).

## References

- [1] RIKTE, S., ANDERSSON, M., KRISTENSSON, G. Homogenization of woven materials. *Research report no. TEAT-7074*, Lund University of Technology, Sweden, Sept 1999, 35 pp.
- [2] WHITES, K. W. Applications of homogenization in electromagnetics. In *XXVIIth General Assembly of the International Union of Radio Science*. Maastricht (Netherlands), 2002, 14-24 Aug.
- [3] HOLLOWAY, C. L., SARTO, M. S., HOJANSON, M. Analyzing carbon-fiber composite materials with equivalent-layer models. *IEEE Transactions on Electromagnetic Compatibility*. 2005, vol. 47, no.4, Nov, p. 833 - 844.
- [4] LIU, L., MATITSINE, S. M., ROZANOV, K. M. Effective permittivity of planar composites with randomly or periodically distributed conducting fibers. *Journal of Applied Physics*. 2005, vol. 98, no. 6, p. 7.
- [5] JILKOVA, J., RAIDA, Z. Genetic homogenization of composite materials. *Radioengineering*. 2009, vol. 18, no.1, p. 34 - 37.
- [6] JARVIS, J. B. *Transmission/Reflection and Short Circuit line Permittivity Measurements*. National Institute of Standards (NIST) Boulder (Colorado), 1990.
- [7] GHODGAONKAR, K. V., VARADAN, V. V. Waveguide probes for complex permittivity measurement. *IEEE Transactions on Instrumentation and Measurement*. 1990, vol. 39, no. 2, April, p. 387 - 394.
- [8] VARADAN, V. V. Extraction of metamaterial properties from measured S-parameters – effects of measurement accuracy, assumed constitutive models, periodicity and randomness. In *Proceedings of Metamaterial*. Rome (Italy), October 2007.
- [9] WU, T. K. *Frequency Selective Surfaces and Grid Arrays*. 1<sup>st</sup> ed. Norwood: Artech House, 1995.
- [10] GONA, S., KRESALEK, V. Accuracy of multilayer equivalent models for composite laminated materials. Accepted for publication on the "International Conference of Applications of Advanced Electronics (ICEAA 09)". Torino (Italy), 2009, Sept 14-18.
- [11] REZNICEK, Z., RAIDA, Z., JILKOVA J. Analyzing small aircraft model with homogeneous composite material substitutes on HIRF. *EMC Europe workshop 2009*. Athens (Greece), p. 1-4.

## About Authors...

**Stanislav GOŇA** was born in Slavičín in 1976. He received his Ing and PhD degrees from the Brno University of Technology in 1999 and 2004, respectively. Between 2002 and 2006 he was employed as a microwave design engineer in Ramet company, Czech Republic. Since 2006 he has been with Tomas Bata University in Zlin where his current interests include material characterization, Electromagnetic compatibility as well as numerical analysis of microwave structures (MoM in Matlab, FEM in Ansys).

**Vojtěch KŘESÁLEK** was born in Valašské Klobouky in 1952. He received his RNDr and PhD Degree in Physical Optics in 1979 and 1984, respectively. Since his habilitation in 1993 at the Faculty of Technology in Zlin, he was involved with research of electric properties of polymer and composite materials and their impedance spectroscopy. More recently, his interests spanned into properties of nanocomposite materials and metamaterials as well as electromagnetic compatibility.

### Appendix A

In this appendix, the TE-z and the TM-z reflection and transmission coefficients for a one layer dielectric (non-magnetic) slab are given.

SINGLE DIELECTRIC LAYER - TE CASE

$$\gamma_0 = \sqrt{\alpha^2 + \beta^2 - k_0^2}, \quad \gamma_1 = \sqrt{\alpha^2 + \beta^2 - k_1^2}$$

$$M_{TE} = \begin{bmatrix} 1 & -\cosh(\gamma_1 t_1) & -\sinh(\gamma_1 t_1) & 0 \\ 0 & 1 & 0 & -1 \\ \gamma_0 & \gamma_0 \cdot \sinh(\gamma_1 t_1) & \gamma_1 \cdot \cosh(\gamma_1 t_1) & 0 \\ 0 & 0 & \gamma_1 & -\gamma_0 \end{bmatrix}$$

$$b_{TE} = \begin{bmatrix} -1 \\ 0 \\ \gamma_0 \\ 0 \end{bmatrix}, \quad x_{TE} = \text{inv}(M_{TE}) \cdot b_{TE},$$

$$R_{TE} = x_{TE}(1,1)$$

$$T_{TE} = x_{TE}(4,1)$$

where  $\gamma_0$  and  $\gamma_1$  stand for z-directed propagation constant, symbols  $\alpha$  and  $\beta$  are x and y components of the wave vector of the incident wave. These components can be expressed as  $\alpha = k_0 \cdot \sin(\vartheta) \cos(\varphi)$  and  $\beta = k_0 \cdot \sin(\vartheta) \sin(\varphi)$ ,

constants  $\vartheta$  and  $\varphi$  account for incident angles. Dielectric slab is described by the complex propagation constant  $k_1 = k_0 \sqrt{\hat{\epsilon}_{r1}}$ , where  $\hat{\epsilon}_{r1} = \epsilon_{r1}(1 - tg\delta_1)$  is a complex permittivity. Finally, last symbol being used is  $t_1$  which stands for the thickness of the dielectric slab.

SINGLE DIELECTRIC LAYER - TM CASE

$$M_{TM} = \begin{bmatrix} \gamma_0 & -\frac{\gamma_1 \cdot \sinh(\gamma_1 t_1)}{\epsilon_1} & -\frac{\gamma_1 \cdot \cosh(\gamma_1 t_1)}{\epsilon_1} & 0 \\ \epsilon_0 & \epsilon_1 & \epsilon_1 & 0 \\ 0 & 0 & \frac{\gamma_1}{\epsilon_1} & -\frac{\gamma_0}{\epsilon_0} \\ 1 & \cosh(\gamma_1 t_1) & \sinh(\gamma_1 t_1) & 0 \\ 0 & 1 & 0 & -1 \end{bmatrix}$$

$$b = \begin{bmatrix} -\gamma_0 / \epsilon_0 \\ 0 \\ 1 \\ 0 \end{bmatrix}, \quad x_{TM} = \text{inv}(M_{TM}) \cdot b_{TM},$$

$$R_{TM} = x_{TM}(1,1)$$

$$T_{TM} = x_{TM}(4,1)$$

Meaning of all symbols is the same as in case of TE polarized coefficients. Symbol  $\epsilon_1$  stands for the complex permittivity of the dielectric slab ( $\epsilon_1 = \epsilon_0 \hat{\epsilon}_{r1}$ ).